10-19-2007

Zebrafish acid-sensing ion channel (ASIC) 4, characterization of homo- and heteromeric channels, and identification of regions important for activation by H+

Xuanmao Chen
University of New Hampshire, Durham, Xuanmao.Chen@unh.edu

Georg Polleichtner
University of Würzburg

Ivan Kadurin
University of Würzburg

Stefan Grunder
University of Tübingen

Recommended Citation
Chen X, Polleichtner G, Kadurin I, Grunder S. Zebrafish acid-sensing ion channel (ASIC) 4, characterization of homo- and heteromeric channels, and identification of regions important for activation by H+. The Journal of biological chemistry. 2007;282(42):30406-13. doi: 10.1074/jbc.M702229200. PubMed PMID: 17686779.

THE JOURNAL OF BIOLOGICAL CHEMISTRY VOL. 282, NO. 42, pp. 30406–30413, October 19, 2007

Zebrafish Acid-sensing Ion Channel (ASIC) 4, Characterization of Homo- and Heteromeric Channels, and Identification of Regions Important for Activation by H^+*

Received for publication, March 14, 2007, and in revised form, July 30, 2007 Published, JBC Papers in Press, August 7, 2007, DOI 10.1074/jbc.M702229200

Xuanmao Chen, Georg Polleichtner, Ivan Kadurin, and Stefan Gründer[1]

From the Department of Physiology II, University of Würzburg, Röntgenring 9, 97070 Würzburg, Germany

There are four genes for acid-sensing ion channels (ASICs) in the genome of mammalian species. Whereas ASIC1 to ASIC3 form functional H^+-gated Na^+ channels, ASIC4 is not gated by H^+, and its function is unknown. Zebrafish has two ASIC4 paralogs: zASIC4.1 and zASIC4.2. Whereas zASIC4.1 is gated by extracellular H^+, zASIC4.2 is not. This differential response to H^+ makes zASIC4 paralogs a good model to study the properties of this ion channel. In this study, we found that surface expression of homomeric zASIC4.2 is higher than that of zASIC4.1. Surface expression of zASIC4.1 was much increased by formation of heteromeric channels, suggesting that zASIC4.1 contributes to heteromeric ASICs in zebrafish neurons. Robust surface expression of H^+-insensitive zASIC4.2 suggests that zASIC4.2 functions as a homomer and is gated by an as yet unknown stimulus, different from H^+. Moreover, we identified a small region just distal to the first transmembrane domain that is crucial for the differential H^+ response of the two paralogs. This post-TM1 domain may have a general role in gating of members of this gene family.

Acid-sensing ion channels (ASICs)[2] are Na^+ channels that are gated by extracellular H^+. Upon a drop in extracellular pH, ASICs rapidly open, depolarizing the cell, and during sustained acidification they desensitize. The genome of mammals, such as mice and humans, contains four *asic* genes that code for at least six distinct ASIC subunits (1). ASIC subunits contain two transmembrane domains, a large extracellular loop and relatively short intracellular N and C termini (2). Functional ASICs are homo- or hetero-oligomeric assemblies of individual subunits (3–9).

The ASIC1a subunit is broadly expressed throughout the central and peripheral nervous system and contributes to synaptic transmission (10, 11). ASIC1b, a splice variant of ASIC1a, is specifically expressed in the peripheral nervous system and might contribute to the perception of pain (12, 13). ASIC2a is broadly expressed in the brain and contributes to synaptic transmission by the formation of heteromeric channels with ASIC1a (3, 6, 8). ASIC2b, a splice variant of ASIC2a, does not generate functional channels on its own but forms heteromeric channels with other ASIC subunits, notably ASIC3 (14). ASIC3, like ASIC1b, is specifically expressed in the peripheral nervous system (15), and there is evidence for a role in the perception and processing of painful stimuli (16–19). ASIC4 has the most restricted expression of all ASIC subunits. In humans, ASIC4 mRNA is strongly expressed only in the pituitary gland; expression in other parts of the brain is faint (20). Like ASIC2b, ASIC4 does not form a functional homomeric channel (20, 21), and unlike ASIC2b, it does apparently also not form functional heteromeric channels with other ASIC subunits (20). These properties distinguish ASIC4 from other ASIC subunits, and, whereas possible functions are emerging for all other ASIC subunits, the function of ASIC4 is still unknown.

Recently, we have reported the cloning of a family of ASICs from the zebrafish (22). Like their mammalian homologs, zASICs are broadly expressed in the zebrafish central nervous system (22). We identified six ASIC subunits, zASIC1.1, 1.2, 1.3, 2, 4.1, and 4.2, that are encoded by six different genes (22). zASIC1.2 and 1.3 are paralogs of zASIC1.1, and zASIC4.2 is a paralog of zASIC4.1, respectively. The existence of paralogs in zebrafish can be at least partly explained by the fish-specific genome duplication in ray-finned fish that happened ~350 million years ago (23). The amino acid sequences of zASIC4.1 and 4.2 are 68% identical; within the ectodomains identity is even 83%. Unlike rat ASIC4, zASIC4.1 forms a functional homomeric channel that is gated by extracellular H^+ with half-maximal activation at pH ~5.8 (22). Moreover, and in contrast to all other zASICs, prolonged acid activation of zASIC4.1 induces a sustained current component. In contrast to zASIC4.1 but similar to rat ASIC4, zASIC4.2 is insensitive to H^+ stimulation (22). It is not known whether zASIC4.1 and 4.2 form heteromeric channels with other zASIC subunits.

In this study, we asked whether surface expression can explain why zASIC4.1 is H^+-sensitive and zASIC4.2 H^+-insensitive. Surprisingly, we found that homomeric zASIC4.2 is much more abundant on the cell surface than zASIC4.1. Both subunits form functional heteromeric channels with new properties by association with another zASIC subunit; surface expression of zASIC4.1 is largely increased by this association. Moreover, we used zASIC4.1 and 4.2 as a model to identify domains that are important for activation by H^+. We identified two such domains. One, a N-terminal domain that is unique to ASIC4, was important for the unique sustained current compo-

* This work was supported by Grant GR 1771 from the Deutsche Forschungsgemeinschaft (to S. G.). The costs of publication of this article were defrayed in part by the payment of page charges. This article must therefore be hereby marked "*advertisement*" in accordance with 18 U.S.C. Section 1734 solely to indicate this fact.

[1] To whom correspondence should be addressed. Tel.: 49-931-31-6046; Fax: 49-931-31-2741; E-mail: stefan.gruender@uni-wuerzburg.de.

[2] The abbreviations used are: ASIC, acid-sensing ion channel; zASIC, zebrafish ASIC; HA, hemagglutinin; VSV-G, vesicular stomatitis virus glycoprotein; MES, 2-(*N*-morpholino)ethanesulfonic acid; RLU, relative light unit.

nent. Another one, the post-TM1 domain, accounted for the differential activation by H^+ of zASIC4.1 and 4.2.

EXPERIMENTAL PROCEDURES

Electrophysiology—cDNAs for zASICs have been previously described (22). Chimeric and mutant channels were generated by recombinant PCR using standard protocols with Pwo DNA polymerase (Roche Applied Science). All PCR-derived fragments were entirely sequenced.

Part of the ovaries of adult *Xenopus laevis* females were surgically removed under anesthesia. Anesthetized frogs were killed after the final oocyte collection by decapitation. Animal care and experiments followed approved institutional guidelines at the Universities of Tübingen and Würzburg.

The follicular membrane was removed by digestion with collagenase type II (Sigma; 1 mg ml^{-1}) for 60–120 min. Synthesis of cRNA, maintenance of *X. laevis* oocytes, and recordings of whole cell currents were done as previously described (24). For expression of homomeric zASICs, we injected 1.5–4 ng of zASIC cRNA. For co-expression of subunits, we injected equal amounts of cRNAs of the two individual subunits, absolute amounts being 0.2 ng (zASIC4.1/1.3) and 4 ng (zASIC4.2/1.3), respectively. Bath solution for two-electrode voltage-clamp contained 140 mM NaCl, 1.8 mM $CaCl_2$, 1.0 mM $MgCl_2$, 10 mM HEPES. For the acidic test solutions, HEPES was replaced by MES buffer. If not specified differently, the membrane potential was clamped to −70 mV. All of the measurements were performed at room temperature (20–25 °C).

Outside-out patch-clamp measurements were performed as previously described (25). Gravity-driven conditioning and activation solution had the same composition as for whole oocyte recordings. The patches were clamped to −70 mV, and the experiments conducted at room temperature.

Determination of Surface Expression—The hemagglutinin (HA) epitope (YPYDVPDYA) of influenza virus was inserted in the extracellular loop of zASIC4.1 between residues Asp^{152} and Leu^{153} and in the loop of zASIC4.2 between residues Glu^{156} and Leu^{157}. Surface expression was determined as previously described (25). The oocytes were injected with 4 ng cRNA of each subunit. Relative light units (RLUs)/s were calculated as a measure of surface-expressed channels. RLUs of HA-tagged channels were at least 200-fold higher than RLUs of untagged channels (zASIC4.1). The results are from two independent experiments with oocytes from two different frogs; at least six oocytes were analyzed for each experiment and each condition.

Co-immunoprecipitation—Co-immunoprecipitation was performed as described in Ref. 22. Briefly, the zASIC4.1 and 4.2 subunits were tagged at their C termini with the vesicular stomatitis virus glycoprotein (VSV-G) epitope, and zASIC1.3 was tagged at its N terminus with the HA epitope. The tagged subunits were co-injected in *Xenopus* oocytes, and microsomal membranes were prepared. Digitonin-solubilized membrane proteins were then immunoprecipitated using an anti-VSV-G antibody, and the immunoprecipitated proteins were analyzed by Western blot using an anti-HA antibody.

Data Analysis—The data were analyzed with the software IgorPro (Wave metrics, Lake Oswego, OR). For each experiment, the oocytes from at least two different batches of frogs were used. For whole oocyte currents, pH response curves (for proton activation) were fitted with a Hill function, $I = r + (I_{max} - r)/(1 + (pH_{50}/[H^+])^a)$, where I_{max} is the maximal current, r is the residual current, pH_{50} is the pH at which half-maximal activation is achieved, and a is the Hill co-efficient. Before fitting, the currents from each measurement were normalized to the value obtained with the lowest pH used. Desensitization of zASIC currents was fitted with a mono-exponential function. The results are reported as the means ± S.E. They represent the means of n individual measurements on different oocytes. Statistical analysis was done with the unpaired t test.

RESULTS

Characterization of the Sustained Current Component of zASIC4.1—As previously reported (22), prolonged application of an acidic solution (pH 5.0) to oocytes expressing zASIC4.1 induced a biphasic current (Fig. 1*A*). A first transient current component developed with no apparent delay and desensitized within less than a second. This component was similar to the typical transient ASIC current. A second component developed during the first few seconds after application of the acidic solution. This component did not desensitize. Although the reversal potential for the transient component is +56 mV (22), the reversal potential for the sustained component was −4 ± 4 mV ($n = 6$; Fig. 1*A*). Hence, whereas the transient component was highly selective for Na^+, the sustained component was unselective. The two components could also be differentiated by their pharmacology. Although 0.5 mM amiloride completely blocked the transient current component, the sustained component was only slightly blocked (Fig. 1*B*). Zn^{2+} (0.5 mM), which affects some ASIC currents (26, 27), completely blocked the sustained component but did not affect the transient component (Fig. 1*B*). Both current components were not observed in water-injected control oocytes (Fig. 1*B*).

The amplitude of the transient zASIC4.1 current was rather small and highly variable (0.5 ± 0.1 μA, $n = 18$), as was the ratio of the transient and the sustained component; for some zASIC4.1-expressing oocytes, the zASIC4.1 current had almost no transient component, whereas for others, like the one shown in Fig. 1*A*, the transient component had approximately twice the amplitude of the sustained component. Interestingly, after the sustained component was induced, wash-out of the acidic solution with a neutral solution (pH 7.4) induced a small "off-current" that vanished within a few seconds. This off-current was consistently seen and can be explained by a partial inhibition by H^+ of the sustained conductance.

zASIC4 shares with mammalian ASIC4 a domain at the cytoplasmic N terminus. This domain is completely conserved among zebrafish, rat, and human ASIC4 (22); rat ASIC1b and zASIC1.1 have a similar domain that is less conserved (13, 22). We asked whether this domain influences the electrophysiological properties of zASIC4.1. We deleted the first 25 amino acids to yield the variant zASIC4.1-M25. For zASIC4.1-M25 the amplitude of the transient peak current was increased ~20-fold (to 9.6 ± 2.4 μA, $n = 5$; Fig. 1*C*). An increased current amplitude after deletion of the N-terminal domain had already been observed for ASIC1b (13). In contrast to the increased transient current component, the sustained current compo-

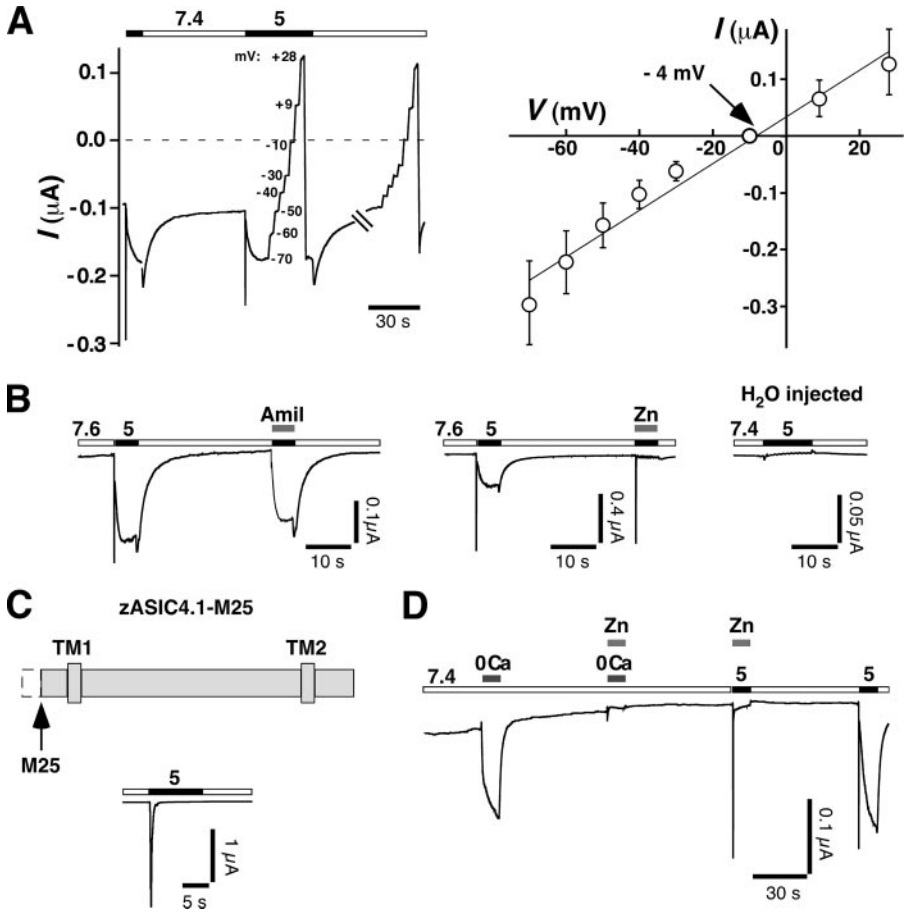

FIGURE 1. **Characteristics of homomeric zASIC4.1.** *A*, *left panel*, representative current trace showing a transient and a sustained current component after application of pH 5 to whole oocytes expressing zASIC4.1. During the sustained phase of the second application, the membrane potential was clamped to different values for 2 s each. Leak currents were determined by the same voltage steps at pH 7.4. *Right panel*, current-voltage relationship for the sustained current component; leak currents had been subtracted from the currents at pH 5 ($n = 6$). *B*, pharmacology of zASIC4.1. *Left panel*, 0.5 mM amiloride (*Amil*) completely blocked the transient current but only slightly blocked the sustained component ($n = 6$). *Middle panel*, 0.5 mM Zn^{2+} completely blocked the sustained current but did not block the transient component ($n = 5$). *Right panel*, application of pH 5 to water-injected oocytes induced neither the transient nor the sustained current component ($n = 4$). Conditioning pH was pH 7.4 or 7.6, as indicated. *C*, representative current trace of N-terminally truncated zASIC4.1-M25 ($n = 5$). The scheme illustrates the position of the truncation. *D*, removal of Ca^{2+} induced the sustained current. All solutions contained 1 mM Mg^{2+}.

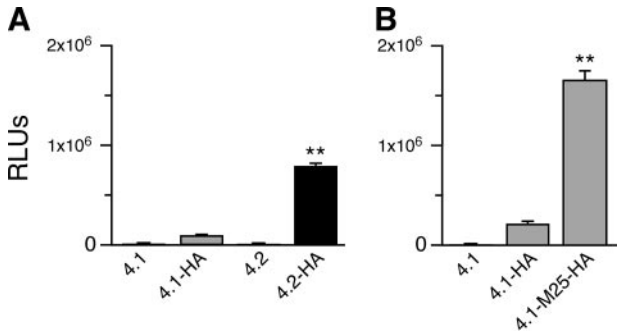

FIGURE 2. **zASIC4.2 but not zASIC4. 1 is robustly expressed on the cell surface.** *A*, surface expression of HA-tagged zASIC4.1 and 4.2 (means ± S.E.). Untagged zASICs served as a control (*first* and *third columns*). The results are expressed as RLUs/oocyte/s. $n = 16–23$; **, $p < 0.01$. *B*, surface expression of HA-tagged zASIC4.1 and zASIC4.1-M25 (means ± S.E.). $n = 14–20$; **, $p < 0.01$.

nent was completely lost (Fig. 1*C*), showing that the unique N-terminal domain of ASIC4 is crucial for the sustained, unselective current component of zASIC4.1. Apparent H^+ affinity of the transient component was not changed by deletion of the N-terminal domain ($pH_{50} = 5.7 \pm 0.1$, $n = 6$ compared with $pH_{50} = 5.7 \pm 0.04$, $n = 9$).

In line with our previous results (22), low pH never elicited a typical transient ASIC current in oocytes expressing zASIC4.2. However, it elicited a sustained current component that developed with a time course similar to that of zASIC4.1 (see Fig. 5). The sustained current component for zASIC4.2 is consistent with the conservation of the N-terminal domain in zASIC4.2. The amplitude of this sustained current, however, was significantly smaller than for zASIC4.1.

We asked whether the sustained current component could be carried by a different channel, for example by a channel activated by Ca^{2+} influx through zASIC4.1 or 4.2. In oocytes expressing zASIC4.1, however, solutions nominally free of Ca^{2+} themselves induced a sustained current ($n = 6$; Fig. 1*D*). This current was blocked by 0.5 mM Zn^{2+} (Fig. 1*D*), had an amplitude comparable with the amplitude of the conductance induced by pH 5, and had a similar reversal potential (-5 ± 1 mV; $n = 6$). Such a conductance was not induced in water-injected oocytes or in oocytes expressing zASIC4.1-M25 (not shown). Thus, this conductance induced by Ca^{2+} removal was related to the presence of zASIC4.1 containing the N-terminal domain. We did not investigate the sustained current further.

Homomeric zASIC4.2 Is Robustly Expressed on the Cell Surface—We next assessed surface expression of zASIC4.1 and 4.2. We inserted an HA epitope into the extracellular loop of both subunits and used a monoclonal anti-HA antibody and a luminescence assay to quantify the surface expression of HA-tagged channels. The luminescence signal of HA-tagged zASIC4.1 was ~200-fold above background of untagged channels (Fig. 2), revealing the presence of homomeric zASIC4.1 channels on the surface. Surprisingly, the luminescence signal of HA-tagged zASIC4.2 was ~10-fold higher than for HA-tagged zASIC4.1 (Fig. 2*A*), showing that zASIC4.2 is robustly expressed at the cell surface; apparently, these surface-expressed channels are not gated by H^+. Moreover, the large luminescence suggests that zASIC4.2 more readily associates with like subunits into homomeric channels than zASIC4.1 and/or that homomeric zASIC4.2 is more efficiently targeted to the plasma membrane than homomeric zASIC4.1.

TABLE 1

Electrophysiological properties of zASICs

The data are the means ± S.E. for the number (*n*) of individual oocytes or individual patches indicated in parentheses. Maximal peak current amplitudes (Peak ampl.) were measured at a saturating pH as indicated. pH values at which channels were half-maximally activated (pH_{50}) and the Hill number *a* were obtained by fitting the pH response curves with the Hill function. Desensitization time constants (τ_{des}) were obtained from outside-out patch clamp recordings with fast solution exchange; individual recordings from 8–12 independent patches were pooled, and the resulting curve was fit with a single exponential function. ND, not determined.

	Peak ampl.	pH_{50}	Hill number *a*	τ_{des}
	μA			*ms*
zASIC1.3	2.2 ± 0.4 (14), pH 5.8	6.57 ± 0.04 (16)	4.6 ± 0.4 (16)	40
zASIC4.1	0.2 ± 0.1 (9), pH 4.8	5.70 ± 0.04 (9)	2.0 ± 0.2 (9)	37
zASIC1.3/4.1	17.9 ± 2.4 (16), pH 5.8[a]	6.71 ± 0.02 (12)[a]	3.3 ± 0.2 (12)[a]	42
zASIC1.3/4.2	6.5 ± 1.4 (14), pH 5.4[a]	6.18 ± 0.05 (15)[a]	1.9 ± 0.1 (15)[a]	ND

[a] Values from oocytes expressing two zASIC subunits that were significantly different ($p < 0.05$) from values from oocytes expressing either of the two subunits alone.

Deletion of the N-terminal domain in zASIC4.1-M25 increased surface expression ~8-fold ($p < 0.01$; Fig. 2*B*), indicating that the increased peak current amplitude with this variant can at least partially be explained by increased surface expression.

zASIC4.1 and zASIC4.2 Form Heteromeric Channels with Other zASIC Subunits—We addressed the issue of plasma membrane trafficking further by investigating whether zASIC4.1 and 4.2 form functional heteromeric channels. Most ASICs readily form heteromeric ion channels (7, 22). An exception is rat ASIC4; co-expression of rat ASIC4 with other ASIC subunits does not give rise to H^+-gated currents with new properties (20). We investigated formation of heteromeric channels with zASIC1.3 because the mRNA for this subunit shows an overlapping expression pattern with zASIC4.1 and 4.2 in the zebrafish central nervous system (22). Fig. 3*A* and Table 1 show that co-expression of zASIC4.1 and 1.3 robustly increased ASIC peak currents (17.9 ± 2.4 μA, $n = 16$, compared with 0.2 ± 0.1 μA, $n = 9$, for zASIC4.1, and 2.2 ± 0.4 μA, $n = 14$, for zASIC1.3). Because this increase in the current amplitude was larger than expected for the simple addition of current amplitudes, it suggested formation of heteromeric channels. Moreover, the luminescence signal of zASIC4.1 was strongly increased (~15-fold) when zASIC4.1 was co-expressed with zASIC1.3 (Fig. 3*A*), suggesting that the increased current amplitude was due to an increased abundance of channels at the cell surface.

The pH response curve of oocytes co-expressing zASIC4.1 and 1.3 could be well fit with the Hill function only when assuming a single group of channels, yielding a pH_{50} of 6.7 ± 0.02 ($n = 12$; Fig. 3*B* and Table 1). Similar to a previous report (22), oocytes expressing zASIC1.3 or zASIC4.1 alone were less sensitive to H^+, with pH_{50} values of 6.6 ± 0.04 ($n = 16$) or 5.7 ± 0.04 ($n = 9$), respectively. The unique H^+ affinity of oocytes co-expressing zASIC4.1 and 1.3 also indicated the formation of heteromeric channels. We confirmed the formation of heteromeric zASIC4.1/1.3 by co-immunoprecipitation (Fig. 3*C*). Together, our results suggest that zASIC4.1 assembles with zASIC1.3 into heteromeric channels. These heteromeric channels are more efficiently targeted to the plasma membrane than the individual subunits and have unique electrophysiological characteristics. Hence, zASIC4.1, like most other ASIC subunits but unlike rat ASIC4, readily forms heteromeric channels.

We then investigated formation of heteromeric channels by zASIC4.2 and zASIC1.3. Co-expressing zASIC4.2 with 1.3 doubled the amplitude of currents obtained with zASIC1.3 alone (6.5 ± 1.4 μA, $n = 14$, compared with 2.2 ± 0.3 μA, $n = 20$; Fig. 4*A* and Table 1). Moreover, the pH response curve of oocytes co-expressing zASIC1.3 and 4.2 was significantly different from the pH response curve of oocytes expressing zASIC1.3 alone ($pH_{50} = 6.2 \pm 0.05$, $n = 15$, compared with $pH_{50} = 6.6 \pm 0.04$, $n = 16$; $p < 0.01$; Fig. 4*B* and Table 1), providing further evidence for a heteromer formed by zASIC4.2 and 1.3. We expected that the incorporation of the silent zASIC4.2 subunit into a functional heteromeric channel might change the cooperativity of the response to H^+. Indeed, the pH response curve of the heteromeric channel was flatter than that of homomeric zASIC1.3 (Fig. 4*B*), and fit with the Hill function yielded a significantly ($p < 0.01$) smaller Hill number *a* for the heteromer ($a = 1.9 \pm 0.1$, $n = 15$) than for the homomer ($a = 4.6 \pm 0.04$, $n = 16$; Table 1). This result suggests that less H^+ cooperated to activate the heteromeric channel. Co-immunoprecipitation confirmed physical association of zASIC4.2 with zASIC1.3 (Fig. 3*C*). Together, these results demonstrate that zASIC4.2 assembles with zASIC1.3 into heteromeric channels. The zASIC4.2/1.3 channel was clearly targeted to and expressed at the plasma membrane.

Oocytes co-expressing either zASIC1.3/4.1 or zASIC1.3/4.2 did not show the sustained current component that is characteristic for homomeric zASIC4, suggesting that the heteromeric channels do not promote this conductance.

Identification of a Short Region Determining the Differential Response to H^+ of zASIC4.1 and zASIC4.2—Finally, using a chimeric approach, we addressed which structural differences account for the presence of a transient peak current with zASIC4.1 and its absence with zASIC4.2. Fig. 5 shows a schematic representation of the chimeras and their response to H^+. We first substituted the cytosolic N terminus of zASIC4.1 with the one from zASIC4.2 (chimera C1). C1 was active, generating ~50-fold larger peak currents than wild-type zASIC4.1 ($n = 14$). This result indicates that the cytosolic N terminus does not account for the differential H^+ response of zASIC4.1 and 4.2; the largely increased current amplitude, however, indicates that the N terminus of zASIC4.2 confers increased surface expression. In chimera C2, we moved the N terminus plus TM1 of zASIC4.2 to substitute the corresponding part of zASIC4.1. C2 was also active ($n = 13$), generating larger current amplitudes than zASIC4.1 but smaller amplitudes than C1. Chimera C3 was composed of the N terminus, TM1, and the proximal one-third of the ectodomain of zASIC4.2, with the rest coming from zASIC4.1. As shown in Fig. 5, C3 did not generate any typical ASIC currents in response to low pH stimulation ($n = 24$). To

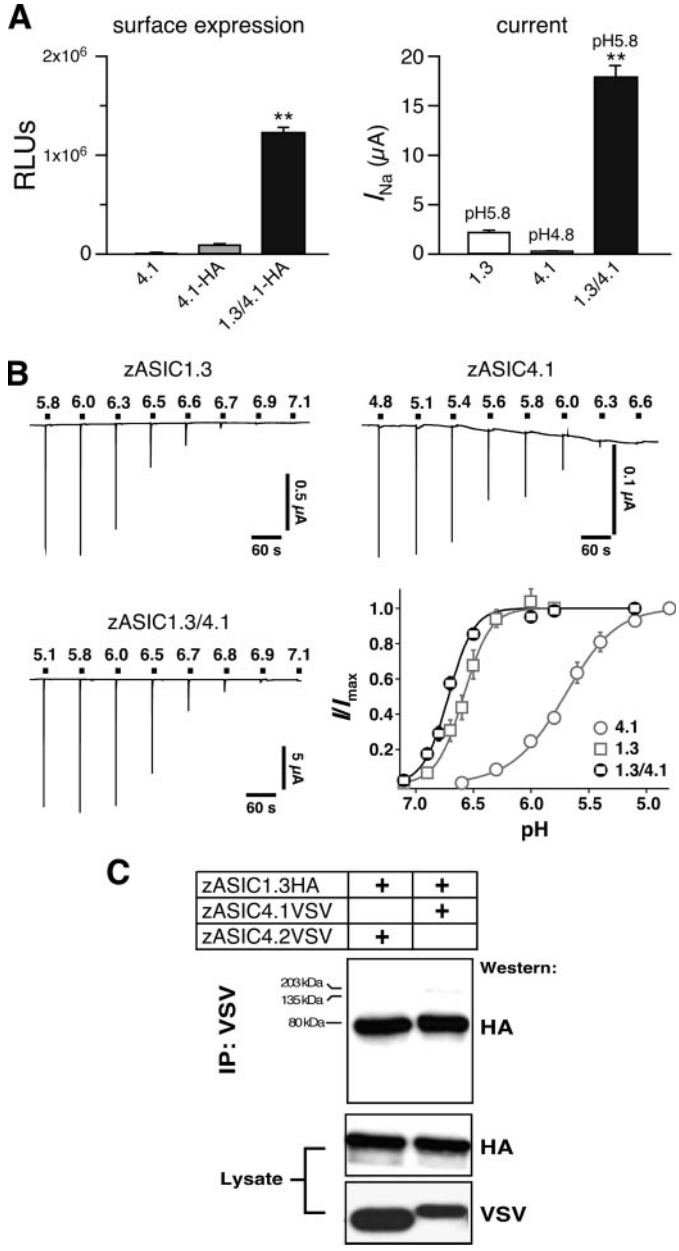

FIGURE 3. **zASIC4.1 forms a functional heteromeric channel with zASIC1.3.** *A*, *left panel*, surface expression of HA-tagged zASIC4.1 or zASIC4.1 co-expressed with zASIC1.3 (means ± S.E.); only zASIC4.1 was tagged with the HA epitope. Untagged zASIC4.1 served as a control (*first column*). The results are expressed as RLUs/oocyte/s. $n = 16$. The results for HA-tagged and untagged zASIC4.1 are from Fig. 2*A*. *Right panel*, peak current amplitude (means ± S.E.) of whole oocytes expressing zASIC1.3 (pH 5.8, $n = 14$), zASIC4.1 (pH 4.8, $n = 9$), or zASIC1.3/4.1 (pH 5.8, $n = 16$). The amounts of cRNA that had been injected into each oocyte were 4 ng of zASIC1.3 or zASIC4.1 or 0.2 ng of zASIC4.1 plus 0.2 ng of zASIC1.3. **, $p < 0.01$. *B*, representative current traces of whole oocytes either expressing zASIC1.3, zASIC4.1, or co-expressing zASIC1.3 and 4.1. The channels were activated for 10 s by varying low pH, as indicated. Conditioning pH 7.4 was applied for 60 s. *Bottom right panel*, pH response curves; the *lines* represent fits to the Hill function. *C*, zASIC4.1 and 4.2 co-precipitate zASIC1.3. Two different zASIC subunits were co-injected in *Xenopus* oocytes as indicated. zASIC4.1 and 4.2 were precipitated using the anti-VSV-G antibody, and co-precipitated zASIC1.3 was detected in the Western blot using the anti-HA antibody. Western blots of the cell lysates, demonstrating the presence of the expected proteins, are shown at the *bottom*. Under these experimental conditions, immunoprecipitation (*IP*) with the anti-VSV-G antibody gives no unspecific background (22).

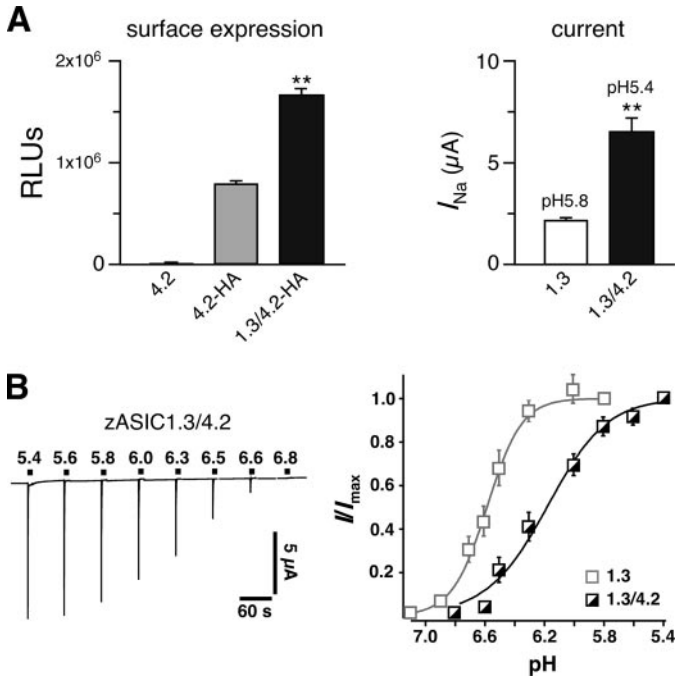

FIGURE 4. **zASIC4.2 forms a functional heteromeric channel with zASIC1.3.** *A*, *left panel*, surface expression of HA-tagged zASIC4.2 and zASIC4.2 co-expressed with zASIC1.3 (means ± S.E.); only zASIC4.2 was tagged with the HA epitope. Untagged zASIC4.2 served as a control (*first column*). The results are expressed as RLUs/oocyte/s. $n = 23$. The results for HA-tagged and untagged zASIC4.2 are from Fig. 2*A*. *Right panel*, peak current amplitude (means ± S.E.) of whole oocytes expressing zASIC1.3 (pH 5.8, $n = 20$) or zASIC1.3/4.2 (pH 5.4, $n = 14$). The amounts of cRNA that had been injected into each oocyte were 4 ng of zASIC1.3 or 4 ng zASIC4.2 plus 4 ng of zASIC1.3. **, $p < 0.01$. *B*, *left panel*, representative current traces of whole oocytes co-expressing zASIC1.3 and 4.2. The channels were activated for 10 s by varying low pH, as indicated. Conditioning pH 7.4 was applied for 60 s. *Right panel*, pH response curves; *lines* represent fits to the Hill function.

corroborate this result, we generated chimera C4, in which only the proximal one third of the ectodomain came from zASIC4.2 and the rest, including the cytoplasmic N terminus and TM1, originated from zASIC4.1. Like C3, C4 did not generate an ASIC current in response to low pH stimulation ($n = 26$). To further confirm the importance of the proximal part of the ectodomain, we constructed chimera C5, which was opposite to C4; we transferred only the proximal one-third of the ectodomain of H^+-sensitive zASIC4.1 to H^+-insensitive zASIC4.2. Indeed, C5 formed a H^+ gated channel, generating ~4 μA ($n = 12$) current upon acidification, which was larger than zASIC4.1 currents. These data show that the proximal part of the ectodomain is critical for the differential H^+ response of zASIC4.1 and 4.2. To further define this critical region, we constructed chimera C6, which was similar to C3 and exchanged the cytoplasmic N terminus, TM1, but only the first 34 amino acids of the ectodomain. C6 was silent ($n = 8$). We then constructed chimera C7, in which only the first 24 amino acids of the ectodomain were exchanged; but this time we transferred this region from zASIC4.1 to 4.2. Chimera C7 indeed formed functional H^+-activated channels ($n = 9$), suggesting that a small region following TM1 is sufficient to explain the differential H^+ response of zASIC4.1 and 4.2. All of the chimeras developed a sustained current component (Fig. 5). The amplitude of this component was variable, but generally it was rather small, like for zASIC4.2, and not as large as for zASIC4.1.

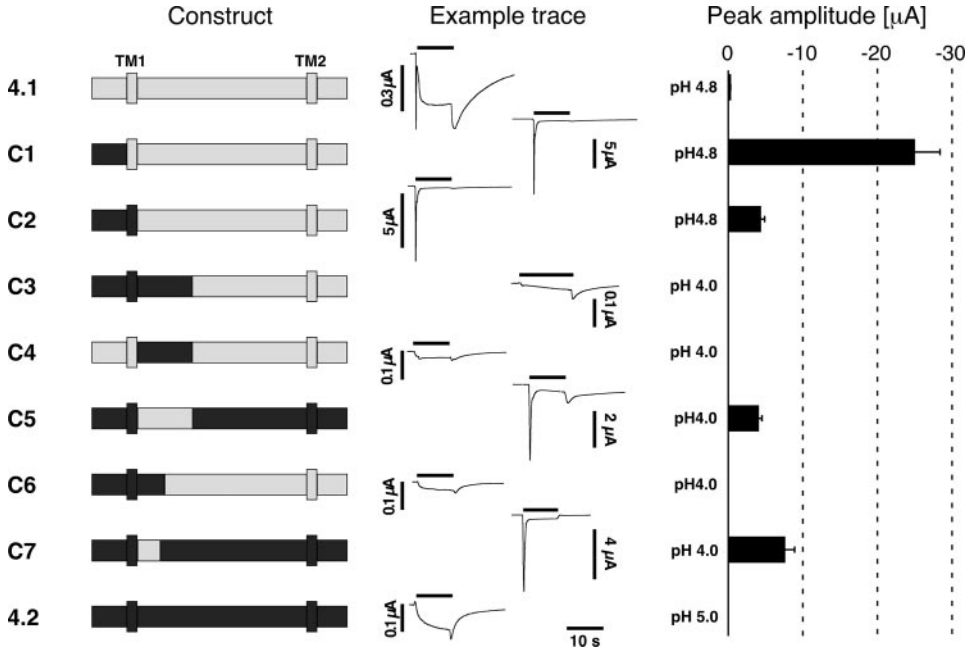

FIGURE 5. **Identification of the region explaining the differential response to H^+ of zASIC4.1 and 4.2.** *Left panel*, schemes of wild-type and chimeric channels. *Middle panel*, representative current traces for each construct. The channels were activated for 10 s by acidic solutions; pH is indicated on the *right*. *Right panel*, peak current amplitudes (means ± S.E.) of whole oocytes; only the transient current was analyzed.

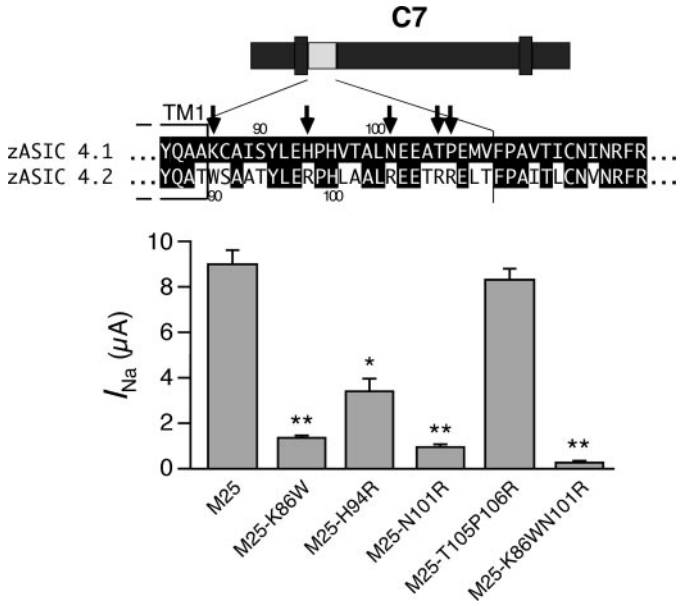

FIGURE 6. **The role of individual amino acids for the differential response to H^+ of zASIC4.1 and 4.2.** *Top panel*, sequence alignment of the proximal part of the ectodomain of zASIC4.1 and 4.2. The positions chosen to make chimera C7 are indicated. Amino acids identical to zASIC4.1 are shown as *white letters* on *black background*. Amino acids substituted are highlighted by an *arrow*. *Bottom panel*, peak current amplitudes (means ± S.E.) of zASIC4.1-M25 and the substituted variants in whole oocytes. *, $p < 0.05$; **, $p < 0.01$.

Contribution of Individual Amino Acids for the Differential Response to H^+ of zASIC4.1 and zASIC4.2—Fig. 6 shows a sequence alignment of the critical region identified by the chimeras. Of the 24 amino acids exchanged in chimera C7, 13 are different and 11 are identical between zASIC4.1 and 4.2. Among the 13 amino acids that are different, only five are clear nonconservative changes, four of them being positively charged arginines in zASIC4.2 and neutral amino acids or a histidine in zASIC4.1. We individually exchanged all of the five nonconserved amino acids in zASIC4.1 by the amino acids found in zASIC4.2 at the corresponding position (K86W, H94R, N101R, and T105R/P106R); the two adjacent residues Thr^{105} and Pro^{106} were exchanged together. The resulting mutant zASIC4.1 channels were silent and could no longer be activated by H^+ (not shown). To exclude that the inactivity of the mutant channels was due to low surface expression of zASIC4.1, we introduced the same amino acid substitutions also in the zASIC4.1-M25 variant. Indeed, now all the mutants were active and generated typical transient ASIC currents, albeit with up to 10-fold smaller current amplitude than zASIC4.1-M25 (Fig. 6). Substitutions K86W and N101R most strongly reduced the current amplitude, suggesting that these two positions are most critical in determining the response to H^+. Therefore, we introduced these two substitutions also together. The resulting mutant zASIC4.1-M25-K86WN101R had a more than 30-fold smaller current amplitude than zASIC4.1-M25 (Fig. 6) but still generated discernible transient ASIC currents.

We then did the inverse substitution, substituting amino acids Trp^{90} and Arg^{105} of zASIC4.2 by the amino acids found in zASIC4.1 (zASIC4.2W90KR105N). However, the substitution of the two critical amino acids together was not sufficient to render zASIC4.2 proton-sensitive (not shown). Therefore, we obtained no evidence that individual amino acids determine the differential response to H^+ of zASIC4.1 and 4.2.

DISCUSSION

This study has two major findings. First, we show that zASIC4.2 is a surface-expressed ion channel that is insensitive to H^+. Second, we identify a small region in the proximal extracellular loop where a few substitutions of amino acids can render an ASIC insensitive to H^+.

Homo-oligomeric zASIC4.2 and Its Function—The strong luminescence of HA-tagged zASIC4.2 (Fig. 2) indicates that this channel is robustly expressed on the cell surface. We assume that only properly folded oligomeric ASICs reach the cell surface; this suggests that zASIC4.2 forms homo-oligomeric channels *in vivo*. Currently we can only speculate about the gating mechanism and function of such homo-oligomeric zASIC4.2.

Because many ASICs are modulated by peptides (24, 28) and a related channel from mollusks, FaNaC, is directly gated by a neuropeptide (29), peptides are attractive candidates for a ligand gating zASIC4.2. The strong expression in pituitary gland of the RNA for rat ASIC4 (20) also makes peptides attrac-

tive candidates for the rat ASIC4 ligand. However, at present no peptides directly activating an ASIC are known.

zASIC4.1 and Its Function—Homomeric zASIC4.1 is a functional H^+-gated ion channel. Surface expression of this channel was low, however, suggesting that homomeric zASIC4.1 may not be of great relevance in zebrafish neurons. It rather seems that zASIC4.1 contributes to functional ASICs by formation of heteromeric channels; our study identifies zASIC1.3 as one likely partner. Based on the overlapping expression pattern of ASICs in the zebrafish central nervous system (22), there may be other partners as well.

The Sustained Current—Among the H^+-sensitive zASICs, zASIC4.1 has the unique property of developing a sustained current after desensitization of the transient current. In this study, we observed a similar sustained current in zASIC4.2-expressing oocytes. The amplitude of this sustained current was highly variable, however, and usually smaller for zASIC4.2 than for zASIC4.1. Because homomeric zASIC4.2 showed an ~10-fold larger surface expression than homomeric zASIC4.1, the amplitude did not correlate with the number of surface-expressed channels. Moreover, the ion selectivity and pharmacology of the sustained current was different from the typical ASIC current. Therefore, it is an open question whether the sustained current was flowing through the ASIC pore.

The sustained current depended on the presence of the N-terminal domain of zASIC4; deletion of this domain abolished the sustained current (Fig. 1). Rat ASIC4 has an almost identical N-terminal domain. Moreover, rat ASIC4-expressing oocytes show a sustained current like zASIC4, and deletion of the N-terminal domain of rat ASIC4 abolishes this sustained current.[3] Thus, this N-terminal domain seems to have a conserved function. Rat ASIC1b and zASIC1.1 have N-terminal domains that are not identical but highly similar to the domain of ASIC4. In contrast to ASIC4, these ASICs do not show a sustained current (13, 22). Deletion of the domain in ASIC1b, however, increases the amplitude of the transient current (13) like for zASIC4.1, likely by increasing surface expression. Thus, this domain seems to impair surface expression of some ASIC channels. This was apparently not the case for zASIC4.2, however, which was robustly expressed on the cell surface, although it contains an N-terminal domain with high sequence identity to zASIC4.1. The large current amplitude of chimera C1 (Fig. 5) suggests that the differential effect of the N-terminal domains of zASIC4.1 and 4.2 on surface expression is determined by other sequences within the cytoplasmic N terminus.

Perhaps zASIC4.1 has two gating modes; the first mode would be shared by other ASICs and would support transient H^+-gated currents, and the second mode would support sustained currents that are gated by H^+ and removal of Ca^{2+}. The N-terminal domain would be crucial for the second gating mode; deletion of this domain would allow only the first mode, typical of ASICs. In hippocampal neurons, Ca^{2+}-sensing nonselective cation channels have been described that share some properties with the second gating mode of zASIC4.1; they are activated by removal of extracellular Ca^{2+}, and the current develops slowly (τ = 1s), is sustained, has a reversal potential ~1 mV, and is inhibited by extracellular H^+ (30, 31). A relation of ASIC4 to this current is at present highly speculative, however. In summary, although these observations provide some information on the N-terminal domain, the biological function of this domain remains unclear.

The Role of the Post-TM1 Domain in ASIC Gating—Our study identifies a small region in the post-TM1 domain that is crucial to explain the H^+ insensitivity of zASIC4.2. Probably mutations at many places in the protein will render zASIC4.2 H^+-insensitive. Therefore, our results provide only circumstantial evidence that the post-TM1 domain has a general role in H^+ gating of ASICs. However, a different study also found that the post-TM1 domain is crucial to distinguish H^+-sensitive from H^+-insensitive ASICs (32). Moreover, there is much more circumstantial evidence from other studies that reinforce the idea that the post-TM1 domain plays an important role in the gating of ion channels from the degenerin/epithelial sodium channel gene family. In ASICs, the proximal ectodomain controls apparent H^+ affinity (33), speed of desensitization (34), and inhibition by the spider toxin PcTx1 (35, 36), a gating modifier toxin (37). Proteolytical cleavage of the post-TM1 domain activates epithelial sodium channel (38, 39), a channel related to ASICs. Finally, in the peptide-gated FaNaC, the proximal ectodomain controls apparent affinity to its ligand, FMRFamide (40).

Two amino acids were most crucial in determining the activity of zASIC4.1: Lys^{86} and Asn^{101}. Amino acids at these two sites are highly conserved among proton-sensitive ASICs; most have an Asp or a Glu at the first position and an Asp at the second position. The high conservation highlights the importance of these two sites. The amino acids found in zASIC4.1 conform much better to the consensus for these amino acids than those found in zASIC4.2 (Trp and Arg). Maybe an amino acid with a hydrophilic, charged side chain is necessary at the first position and an amino acid with a hydrophilic negatively charged or neutral side chain is necessary at the second position. Inactivity of zASIC4.2 with the two critical amino acids substituted by those of zASIC4.1 shows, however, that these two amino acids are not the only determinants of proton sensitivity.

The importance of the proximal ectodomain is surprising, because in ASICs it is much less conserved than the distal ectodomain. Perhaps sequence divergence in this region is at the origin of the diverse functions and gating mechanisms of channels in this gene family.

Acknowledgments—We thank M. Siba and P. Seeberger for expert technical assistance and M. Paukert for advice on outside-out patches.

REFERENCES

1. Kellenberger, S., and Schild, L. (2002) *Physiol. Rev.* **82,** 735–767
2. Saugstad, J. A., Roberts, J. A., Dong, J., Zeitouni, S., and Evans, R. J. (2004) *J. Biol. Chem.* **279,** 55514–55519
3. Baron, A., Waldmann, R., and Lazdunski, M. (2002) *J. Physiol.* **539,** 485–494

[3] X. Chen and S. Gründer, unpublished results.

4. Benson, C. J., Xie, J., Wemmie, J. A., Price, M. P., Henss, J. M., Welsh, M. J., and Snyder, P. M. (2002) *Proc. Natl. Acad. Sci. U. S. A.* **99,** 2338–2343
5. Xie, J., Price, M. P., Berger, A. L., and Welsh, M. J. (2002) *J. Neurophysiol.* **87,** 2835–2843
6. Askwith, C. C., Wemmie, J. A., Price, M. P., Rokhlina, T., and Welsh, M. J. (2004) *J. Biol. Chem.* **279,** 18296–18305
7. Hesselager, M., Timmermann, D. B., and Ahring, P. K. (2004) *J. Biol. Chem.* **279,** 11006–11015
8. Vukicevic, M., and Kellenberger, S. (2004) *Am. J. Physiol.* **287,** C682–C690
9. Wu, L. J., Duan, B., Mei, Y. D., Gao, J., Chen, J. G., Zhuo, M., Xu, L., Wu, M., and Xu, T. L. (2004) *J. Biol. Chem.* **279,** 43716–43724
10. Waldmann, R., Champigny, G., Bassilana, F., Heurteaux, C., and Lazdunski, M. (1997) *Nature* **386,** 173–177
11. Wemmie, J. A., Chen, J., Askwith, C. C., Hruska-Hageman, A. M., Price, M. P., Nolan, B. C., Yoder, P. G., Lamani, E., Hoshi, T., Freeman, J. H., Jr., and Welsh, M. J. (2002) *Neuron* **34,** 463–477
12. Chen, C. C., England, S., Akopian, A. N., and Wood, J. N. (1998) *Proc. Natl. Acad. Sci. U. S. A.* **95,** 10240–10245
13. Bässler, E. L., Ngo-Anh, T. J., Geisler, H. S., Ruppersberg, J. P., and Gründer, S. (2001) *J. Biol. Chem.* **276,** 33782–33787
14. Lingueglia, E., de Weille, J. R., Bassilana, F., Heurteaux, C., Sakai, H., Waldmann, R., and Lazdunski, M. (1997) *J. Biol. Chem.* **272,** 29778–29783
15. Waldmann, R., Bassilana, F., de Weille, J., Champigny, G., Heurteaux, C., and Lazdunski, M. (1997) *J. Biol. Chem.* **272,** 20975–20978
16. Sutherland, S. P., Benson, C. J., Adelman, J. P., and McCleskey, E. W. (2001) *Proc. Natl. Acad. Sci. U. S. A.* **98,** 711–716
17. Sluka, K. A., Price, M. P., Breese, N. M., Stucky, C. L., Wemmie, J. A., and Welsh, M. J. (2003) *Pain* **106,** 229–239
18. Sluka, K. A., Radhakrishnan, R., Benson, C. J., Eshcol, J. O., Price, M. P., Babinski, K., Audette, K. M., Yeomans, D. C., and Wilson, S. P. (2007) *Pain* **129,** 102–112
19. Yagi, J., Wenk, H. N., Naves, L. A., and McCleskey, E. W. (2006) *Circ. Res.* **99,** 501–509
20. Gründer, S., Geissler, H. S., Bässler, E. L., and Ruppersberg, J. P. (2000) *Neuroreport* **11,** 1607–1611
21. Akopian, A. N., Chen, C. C., Ding, Y., Cesare, P., and Wood, J. N. (2000) *Neuroreport* **11,** 2217–2222
22. Paukert, M., Sidi, S., Russell, C., Siba, M., Wilson, S. W., Nicolson, T., and Gründer, S. (2004) *J. Biol. Chem.* **279,** 18783–18791
23. Meyer, A., and Van de Peer, Y. (2005) *Bioessays* **27,** 937–945
24. Chen, X., Paukert, M., Kadurin, I., Pusch, M., and Gründer, S. (2006) *Neuropharmacology* **50,** 964–974
25. Chen, X., and Gründer, S. (2007) *J. Physiol.* **579,** 657–670
26. Baron, A., Schaefer, L., Lingueglia, E., Champigny, G., and Lazdunski, M. (2001) *J. Biol. Chem.* **276,** 35361–35367
27. Chu, X. P., Wemmie, J. A., Wang, W. Z., Zhu, X. M., Saugstad, J. A., Price, M. P., Simon, R. P., and Xiong, Z. G. (2004) *J. Neurosci.* **24,** 8678–8689
28. Askwith, C. C., Cheng, C., Ikuma, M., Benson, C., Price, M. P., and Welsh, M. J. (2000) *Neuron* **26,** 133–141
29. Lingueglia, E., Champigny, G., Lazdunski, M., and Barbry, P. (1995) *Nature* **378,** 730–733
30. Xiong, Z., Lu, W., and MacDonald, J. F. (1997) *Proc. Natl. Acad. Sci. U. S. A.* **94,** 7012–7017
31. Chu, X. P., Zhu, X. M., Wei, W. L., Li, G. H., Simon, R. P., MacDonald, J. F., and Xiong, Z. G. (2003) *J. Physiol.* **550,** 385–399
32. Coric, T., Zheng, D., Gerstein, M., and Canessa, C. M. (2005) *J. Physiol.* **568,** 725–735
33. Babini, E., Paukert, M., Geisler, H. S., and Gründer, S. (2002) *J. Biol. Chem.* **277,** 41597–41603
34. Coric, T., Zhang, P., Todorovic, N., and Canessa, C. M. (2003) *J. Biol. Chem.* **278,** 45240–45247
35. Salinas, M., Rash, L. D., Baron, A., Lambeau, G., Escoubas, P., and Lazdunski, M. (2006) *J. Physiol.* (*Lond.*) **570,** 339–354
36. Chen, X., Kalbacher, H., and Gründer, S. (2006) *J. Gen. Physiol.* **127,** 267–276
37. Chen, X., Kalbacher, H., and Gründer, S. (2005) *J. Gen. Physiol.* **126,** 71–79
38. Hughey, R. P., Bruns, J. B., Kinlough, C. L., Harkleroad, K. L., Tong, Q., Carattino, M. D., Johnson, J. P., Stockand, J. D., and Kleyman, T. R. (2004) *J. Biol. Chem.* **279,** 18111–18114
39. Bruns, J. B., Carattino, M. D., Sheng, S., Maarouf, A. B., Weisz, O. A., Pilewski, J. M., Hughey, R. P., and Kleyman, T. R. (2007) *J. Biol. Chem.* **282,** 6153–6160
40. Cottrell, G. A., Jeziorski, M. C., and Green, K. A. (2001) *FEBS Lett.* **489,** 71–74

Zebrafish Acid-sensing Ion Channel (ASIC) 4, Characterization of Homo- and Heteromeric Channels, and Identification of Regions Important for Activation by H^+

Xuanmao Chen, Georg Polleichtner, Ivan Kadurin and Stefan Gründer

J. Biol. Chem. 2007, 282:30406-30413.
doi: 10.1074/jbc.M702229200 originally published online August 7, 2007
